Physics Letters A ••• (••••) ••••••

Contents lists available at ScienceDirect

Physics Letters A

www.elsevier.com/locate/pla

Configurational complexity of nonautonomous discrete one-soliton and rogue waves in Ablowitz-Ladik-Hirota waveguide

Pooja Thakur [a], Marcelo Gleiser [b], Anil Kumar [c], Rama Gupta [a,*]

[a] Department of Physics, D.A.V. University, Jalandhar-144 012, Punjab, India
[b] Department of Physics and Astronomy, Darmouth College, Hanover, NH 03755, USA
[c] Department of Physics, JC DAV College (Panjab University), Dasuya-144 205, Punjab, India

ARTICLE INFO

Article history:
Received 8 October 2020
Received in revised form 10 November 2020
Accepted 12 November 2020
Available online xxxx
Communicated by B. Malomed

Keywords:
Configurational complexity
Configurational entropy
Discrete soliton and rogue waves
Optical fiber
Ablowitz-Ladik-Hirota waveguide with variable coefficient

ABSTRACT

We compute the configurational complexity (CC) for discrete soliton and rogue waves traveling along an Ablowitz-Ladik-Hirota (ALH) waveguide and modeled by a discrete nonlinear Schrödinger equation. We show that for a specific range of the soliton transverse direction κ propagating along the parametric time $\zeta(t)$, CC reaches an evolving series of global minima. These minima represent maximum compressibility of information in the momentum modes along the Ablowitz-Ladik-Hirota waveguide. Computing the CC for rogue waves as a function of background amplitude modulation μ, we show that it displays two essential features: a maximum representing the optimal value for the rogue wave inception (the "gradient catastrophe") and saturation representing the rogue wave dispersion into constituent wave modes. We show that saturation is achieved earlier for higher values of modulation amplitude as the discrete rogue wave evolves along time $\zeta(t)$.

1. Introduction

The discrete nonlinear Schrödinger (DNLS) equation, the discrete version of the continuous nonlinear Schrödinger (NLS) equation, models the dynamics of various oscillatory physical systems, including nonlinear waveguide arrays and nonlinear lattices [1]. It is well-known that both discrete and continuous equations have wide applicability in many areas of physics, from nonlinear optics and plasma physics to hydrodynamics and biology [2–4]. An incomplete list of applications of the DNLS equation includes light propagation arrays on optical waveguides [5–7], Bose-Einstein condensates (BECs) trapped in deep optical lattices [8], denaturation of the DNA double strand [9], breathers in granular crystals [10], dynamics of protein loops [11], molecular crystals [12], and atomic chains [13]. The Ablowitz-Ladik-Hirota (ALH) equation is a finite-difference approximation to the NLS and thus plays a significant role in the study of anharmonic lattices [3,14]. Its various applications include rogue [15,16] and solitary waves [17], as well as Bloch oscillations [18] among others.

In this paper, we will focus our attention on discrete solitons modeled by the ALH equation, examining their stability as applied to their propagation on nonlinear wave guides [19]. In 1973, it was shown that optical solitons in a fiber behave as solitary waves with envelope satisfying the NLS equation. This theoretical prediction was observed experimentally in 1980 [20], with solitons clearly forming on waveguides. In turn, the use of DNLS equation as an approximate model gained importance particularly in the area of AlGaAs waveguide arrays [21].

Of particular interest is the study of localized excitations solutions of the DNLS equation. Among these wave excitations one finds rogue waves [15]–also known as freak waves–sudden, spontaneously-emerging surface waves which may occur in deep oceans and shallow waters, with potentially disastrous consequences [15,16]. Rogue waves have been observed in various physical systems, including nonlinear optical fibers [22–24], superfluids [25,26], Bose-Einstein condensates [27], and capillary waves [26,28].

Various strategies are adopted to extract the dynamical features of physical systems modeled by the DNLS equation, including the AL model [3] and the Salerno model [29]. In this work, we propose to expand the investigation of such configurations by using Configurational Complexity (CC), one of a family of Configuration Information Measures (CIMs) designed to study spatial complexity and stability of spatially-localized discrete or continuous configurations that emerge in many different areas of physics, including various solitons in the NLS equation and its discrete versions. Inspired by Shannon information theory [30], CIMs make use of the

* Corresponding author.
E-mail addresses: poojaphy19@gmail.com (P. Thakur), Marcelo.Gleiser@dartmouth.edu (M. Gleiser), anilkumarphys@gmail.com (A. Kumar), rama.gupta01@gmail.com (R. Gupta).

https://doi.org/10.1016/j.physleta.2020.127039
0375-9601/

continuous or discrete Fourier transform of square-integrable fields to establish an equivalent information content description whereby the field is a "message" written in terms of its momentum modes k, the "alphabet," which appear with a certain probabilistic frequency.

The first member of the family of CIMs was originally proposed in the work by Gleiser and Stamatopoulos [31], where it was called Configurational Entropy (CE). Since then, it became clear that there are four different entropic and complexity information measures, as defined and explained in the work by Gleiser and Sowinski [32]. In particular, the measure originally used by Gleiser and Stamatopoulos is, in fact, the differential configurational complexity (DCC). ("Differential" is applied when one deals with a continuous function or field.) We define this measure below, but refer the reader to Ref. [32] for details.

For the case of discrete solitons and rogue waves, the appropriate CIM is CC [32]. There is a firm link between information and dynamics, where the entropic computations signal the emergence of nonlinear structures and highlight their stability properties [31,33]. CIMs have been applied to a wide variety of physical systems, such as neutron and boson stars [34], spontaneous symmetry breaking [33] and criticality during phase transitions [35], glueballs [36], Q-balls [37], anti-de Sitter black holes [38,39], graviton Bose-Einstein condensates in the brane-world [40], the energy-energy correlation of e^+e^- into hadrons [41], oscillon lifetimes in scalar field theories [42], instantons and vacuum decay in arbitrary spatial dimensions [32], dynamical tachyonic holographic Ads/QCD models [43], standard model [44] and inflationary cosmology [45], and in the study of dissociation of heavy vector mesons in a thermal medium [46]. Specific solitonic applications include bounces in one spatial dimension and critical bubbles in three spatial dimensions [31], solitons in supersymmetric theories [47], Korteweg-de Vries solitons in quark-gluon plasma [48], transition behavior of the discrete nonlinear Schrödinger equation [49], and optical bright similariton in tapered graded-index waveguides [50].

Here, we apply CC to waves propagating in Ablowitz-Ladik-Hirota (ALH) lattices [51–54], modeled with variable [50] as opposed to constant coefficients [48]. In section 2, we briefly review CC. In section 3, the discrete one-soliton and rogue wave solutions of the DNLS equation are obtained invoking a similarity transformation. First, we show that the discrete soliton CC has global minima as a function of transverse direction κ and time variable $\zeta(t)$, indicating the configurational stability of discrete solitons propagating on a Ablowitz-Ladik-Hirota lattice or waveguide. Second, we examine the solutions for rogue waves as a function of the background amplitude modulation μ, and find two essential features: there is a pronounced maximum for CC representing the "gradient catastrophe" typical of the inception of a rogue wave; also, there is saturation for larger values of μ as CC tends to vanish, which occurs at earlier times as μ increases. Our results are summarized in section 4.

2. Configurational complexity for discrete one-solitons and rogue waves

Consider a scalar field configuration, $\varphi(\mathbf{r})$, within a finite volume V and periodic boundary conditions. The field can be decomposed into a countable sum of Fourier modes

$$\varphi(\mathbf{r}) = \sum_{\mathbf{k}} \tilde{\varphi}_{\mathbf{k}} e^{i\mathbf{k}\cdot\mathbf{r}}. \tag{1}$$

The two-point correlation function contains information about the shape of the field. Its Fourier transform, the power spectrum, encapsulates the strength of all the modes that go into generating the configuration,

$$\frac{1}{V}\int d^d\mathbf{r}'\, \varphi(\mathbf{r}')\varphi(\mathbf{r}'+\mathbf{r}) = \sum_{\mathbf{k}} |\tilde{\varphi}_{\mathbf{k}}|^2 e^{i\mathbf{k}\cdot\mathbf{r}}. \tag{2}$$

Given a specific power spectrum, the relative contribution of different modes is quantified by the *modal fraction*

$$f_{\mathbf{k}} = \frac{|\varphi_{\mathbf{k}}|^2}{\max|\varphi_{\mathbf{k}'}|^2}, \tag{3}$$

which satisfies $0 \le f_{\mathbf{k}} \le 1$. The normalization with the maximum mode guarantees the positivity of the configurational complexity (CC), defined as [31]

$$C_C[\varphi] = -\sum_{\mathbf{k}} f_{\mathbf{k}} \ln f_{\mathbf{k}}. \tag{4}$$

This measure vanishes if all the non-zero modes contributing to a configuration have a uniform modal fraction (i.e., carry the same weight). It also vanishes for a plane wave. Somewhere in between the monotony of a plane wave and the randomness of uncorrelated white noise CC maximizes, lending weight to the interpretation of CC as a measure of shape complexity. Configurational Entropy (CE), on the other hand, maximizes when all modes contribute equally, justifying the use of "entropy." This explains our use of "entropy" and "complexity" for CE and CC, respectively. CE is defined without the normalization by the maximum mode contribution and is thus concerned with quantifying the number of bits necessary to construct a field configuration out of wave modes. (This was not quite clear in the previous literature, as pointed out in Ref. [32]. What was called CE is now called CC.)

3. Configurational complexity for nonautonomous discrete one-solitons and rogue waves

3.1. Model equation and discrete one-soliton solution

Wave propagation in generalized Ablowitz-Ladik Hirota (ALH) lattices with variable coefficients is modeled by the DNLS equation [51–54]. The (1+1) Dimensional form of the DNLS equation is given as

$$i\frac{\partial U_n}{\partial t} + [\lambda(t)U_{n+1} + \lambda^\star(t)U_{n-1}](1+h(t)|U_n|^2) - 2\nu_n(t)U_n + i\alpha(t)U_n + (\zeta(t)-\chi(t))U_n = 0. \tag{5}$$

Here $U_n \equiv U_n(t)$ denotes the complex field amplitude at the nth site of the lattice, with $n = 0, \pm1, \pm2.....$ The complex-valued function $\lambda(t)$ is the coefficient of tunnel coupling between sites and can be rewritten as $\lambda(t) = a(t) + ib(t)$ with $a(t)$ and $b(t)$ being real-valued functions. $h(t)$, $\nu_n(t)$, and $\alpha(t)$ are the time-modulated coefficients of intersite nonlinearity, space and time modulated inhomogeneous frequency shift, and time modulated gain or loss term, respectively. $\chi(t)$ and $\zeta(t)$ are functions of time.

The discrete soliton solution of Eq. (5) can be obtained by transforming it into a standard discrete Hirota equation by using the similarity transformation [51–54]

$$U_n(t) = g(t)\exp[i\phi_n(t)]\Psi_n(\zeta(t)), \tag{6}$$

where the $g(t)$ is the real-valued function of time and the phase $\phi_n(t)$ is a function of space and time.

Assuming the phase is a first degree polynomial in space with time-dependent coefficients,

$$\phi_n(t) = C_1(t)n + C_2(t), \tag{7}$$

and substituting Eqs. (6) and (7) into Eq. (5), a set of first-order differential equations for the parameters of transformation is obtained, and the transformed field Ψ satisfies the standard discrete Hirota equation [55]

$$i\frac{\partial \Psi_n}{\partial \zeta} + \frac{1}{2}[2(A+iB)\Psi_{n+1} + 2(A-iB)\Psi_{n-1}](1+M|\Psi_n|^2) - A\Psi_n = 0, \quad (8)$$

where the parameters are related through a set of nonlinear ordinary differential equations,

$$\dot{g}(t) + \alpha(t)g(t) = 0,$$
$$[\dot{C}_1(t)n + \dot{C}_2(t)] + 2\nu_n(t) - \zeta(t) = 0,$$
$$h(t)[g(t)]^2 = M,$$
$$C_1(t) + \sigma_1(t) = \tan^{-1}(B/A),$$
$$A = \frac{\chi(t)}{\dot{\zeta}},$$
$$\zeta(t) = \frac{2}{A}\int_0^t \cos(\tan^{-1}(B/A))d\tau,$$
$$\chi(t) = 2[a(t)\cos(C_1(t)) + b(t)\sin(C_1(t))].$$

We write the parameters $a(t)$ and $b(t)$ as

$$a(t) = \cos(\sigma_1(t)), b(t) = \sin(\sigma_1(t)).$$

Solving equation for $g(t)$,

$$g(t) = g_0 \exp[\int_0^t \alpha(s)ds],$$

and choosing $\alpha(t) = \alpha_0 \sin(t)^2\cos(t)$, we obtain

$$g(t) = g_0\alpha_0 \exp(-\frac{1}{3}\sin(t)^3).$$

We parameterize the external potential ν_n in Eq. (5) as

$$\nu_n(t) = \nu_1(t)n + \nu_2(t),$$

with

$$\nu_1(t) = -\frac{\dot{C}_1(t)}{2},$$
$$\nu_2(t) = -\frac{\dot{C}_2(t)}{2} + \frac{\zeta(t)}{2}.$$

We further write

$$C_1(t) = \tan(\sin(t) + \cos(t)),$$

so that

$$\dot{C}_1(t) = \sec[\cos(t) + \sin(t)]^2(\cos(t) - \sin(t)),$$

and

$$\nu_n(t) = -\frac{1}{2}\sec[\cos(t) + \sin(t)]^2(\cos(t) - \sin(t)) - \frac{\dot{C}_2(t)}{2} + \frac{2}{A}\cos(\tan^{-1}(B/A))\zeta(\tau),$$
$$h(t) = \frac{M}{g_0 \exp[\int_0^t \alpha(s)ds]},$$
$$\sigma_1(t) = \tan(\sin(t) + \cos(t)) - \tan^{-1}(B/A).$$

Eq. (5) and its transformed version Eq. (8) admit soliton solutions [55], as well as rogue waves and breathers [15]. In particular, writing the transverse direction as κ, the discrete one-soliton solution of Eq. (8) is given as

$$U_n(n,\zeta) = \frac{g}{\sqrt{\epsilon}}\sinh(\frac{\kappa+\kappa^*}{2})\mathrm{sech}\Big(\frac{\kappa+\kappa^*}{2}n + \frac{\xi+\xi^*}{2}\zeta + \log(\frac{\sqrt{\epsilon}}{2}\sinh(\frac{\kappa+\kappa^*}{2}))\Big)e_1e_2, \quad (9)$$

where,

$$e_1 = \exp[i(C_1n + C_2)],$$
$$e_2 = \exp[(\frac{\kappa-\kappa^*}{2}n + \frac{\xi-\xi^*}{2}\zeta)],$$
$$\xi = i\gamma(\cosh(\kappa) - 1) - \beta\sinh(\kappa).$$

Choosing $\kappa^* = 0$, $\xi^* = 0$, for discrete one-soliton solution we obtain,

$$U_n(n,\zeta) = \frac{g}{\sqrt{\epsilon}}\sinh(\frac{\kappa}{2})\mathrm{sech}\Big(\frac{\kappa}{2}n + \frac{\xi}{2}\zeta + \log(\frac{\sqrt{\epsilon}}{2}\sinh(\frac{\kappa}{2}))\Big)e_1e_2. \quad (10)$$

3.2. Calculation of configurational complexity for discrete one-soliton

The position-space energy density corresponding to Eq. (10) is

$$\rho(n,\zeta) = \frac{\kappa}{4}\mathrm{sech}\left(\frac{\kappa}{2}n - \frac{\xi}{2}\zeta + \log(\frac{\sqrt{\epsilon}}{2}\sinh(\frac{\kappa}{2}))\right)^2. \quad (11)$$

After exploring the available parameter space for $\rho(n,\zeta)$, we found that CC depends mainly on the transverse direction κ and time $\zeta(t)$ of the discrete one-soliton. To investigate this dependence, we fix the values of the other parameters as $\gamma = i, \beta = 0.001, \epsilon = 1, g_0 = 1, \alpha_0 = 1, M = 1, A = 2, B = 0$. CC for discrete soliton energy density (given by Eq. (11)) has been obtained using Eq. (4) for several values of $\zeta(t)$ and κ.

Profiles of CC as a function of time parameter for illustrative values of the transverse direction are shown in Fig. 1 and Fig. 2, respectively. In both cases, we observe a clear global minimum value for $C_c(\kappa)$ and $C_c(\zeta(t))$. We also observe plateaus for small and large values of the variables (Fig. 1) and for large values of κ (Fig. 2). The asymptotic high plateaus imply small relative change in the shape complexity of the soliton early and later in time, with higher spatial localization: more momentum modes contribute similarly to the object and there is not much relative gain or loss of efficiency in information storage in time. As discussed in the CIMs literature, a minimum in CC indicates stability (see, e.g., Refs. [35,34,32]). For these configurations in both figures, there is less spatial compression and a larger number of modes contribute to the modal fraction. In practical terms, this allows for more information to be encoded into the one-soliton of the Ablowitz-Ladik lattice.

3.3. Configurational complexity for nonautonomous discrete rogue waves

The nonautonomous discrete one-rogue wave solution of Eq. (8) is given as [15,54],

$$U_n(n,\zeta) = g\sqrt{\mu}\left[(1 - \frac{4(1+\mu)(1+2\iota\mu\zeta)}{1+4\mu n^2+16\mu^2+(1+\mu)\zeta^2})\right]e_1e_7, \quad (12)$$

where μ is the background amplitude and

$$e_1 = \exp[i(C_1n + C_2)],$$
$$e_7 = \exp[i(2\zeta((1+\mu)\sqrt{A^2+B^2} - A) + n\tan^{-1}(B/A)].$$

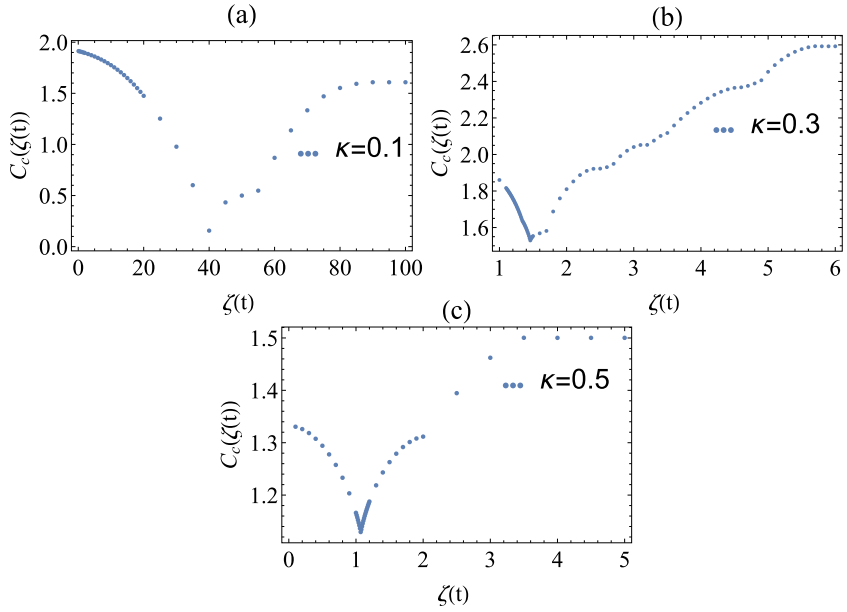

Fig. 1. Configurational complexity of discrete one-soliton $C_c(\zeta(t))$ for several values of transverse direction κ as a function of time variable $\zeta(t)$. The minimum value of $C_c(\zeta(t))$ varies with κ and occurs at (a) $\zeta(t) = 40.0$, (b) $\zeta(t) = 1.47$ and (c) $\zeta(t) = 1.07$ for $\kappa = 0.1, 0.3, 0.5$, respectively.

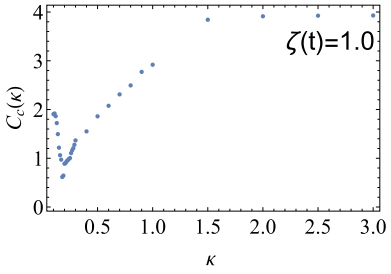

Fig. 2. Snapshot of configurational complexity $C_c(\kappa)$ as a function of transverse direction κ of the discrete one-soliton. The minimum value of CC occurs at $\kappa = 0.18$.

The related position-space energy density is,

$$\rho(n,\zeta) = \frac{\left[\left(1-\frac{4(1+\mu)(1-2\iota\mu\zeta)}{e_8}\right)\left(1-\frac{4(1+\mu)(1+2\iota\mu\zeta)}{e_8}\right)\right]}{\left[1+\frac{8(1+\mu)^2(-\iota+2\mu\zeta)(\iota+2\mu\zeta)}{(e_9)(e_{10})}-\frac{4\sqrt{\mu}(1+\mu)(e_{11})}{(e_9)^{\frac{3}{2}}}\tan^{-1}\left[\frac{2\sqrt{\mu}}{\sqrt{e_9}}\right]\right]}, \tag{13}$$

where

$$e_8 = 1+4n^2\mu+16\mu^2(1+\mu)\zeta^2,$$
$$e_9 = 1+16\mu^2\zeta^2+16\mu^3\zeta^2,$$
$$e_{10} = 1+4\mu+16\mu^2\zeta^2+16\mu^3\zeta^2,$$
$$e_{11} = (-1+12\mu\zeta^2+12\mu^2\zeta^2).$$

Values of the various parameters were fixed as $g_0 = 1, \alpha_0 = 1, M = 1, A = 2, B = 0$. The configurational saturation states have been achieved at $\zeta(t) \simeq 2.1$, 1.0, and 0.62, for values of background amplitude parameter $\mu = 0.1, 0.3$, and 0.5, respectively: for higher values of background amplitude μ, saturation occurs earlier in the propagation time $\zeta(t)$ (Fig. 3) [56].

In terms of CC, we can interpret the rogue wave as the maximum instability solution, thus at strong spatial concentration and thus large CC. At the other extreme (CC $\to$ 0), the saturation state is equivalent to all modes carrying the same weight, representing the dispersion of the wave. In Fig. 4, we show the ranges of

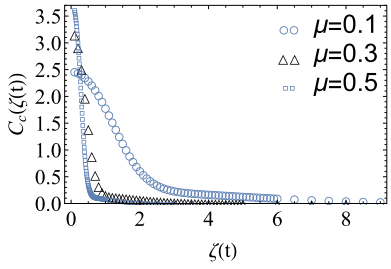

Fig. 3. Configurational complexity $C_c(\zeta(t)$ of discrete one-rogue wave in the Ablowitz-Ladik Hirota (ALH) lattice propagating in the $\zeta(t)$ time with background amplitude $\mu = 0.1, 0.3, 0.5$. Saturation ($C_c(\zeta(t) \to 0$) occurs earlier for larger values of μ.

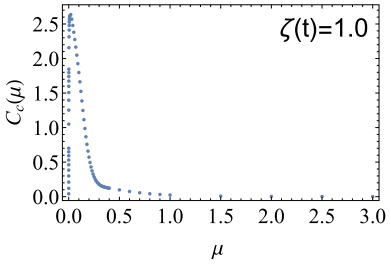

Fig. 4. Snapshot of configurational complexity $C_c(\mu)$ for the discrete one-rogue wave propagating in the Ablowitz-Ladik Hirota (ALH) lattice as a function of the parameter μ, showing a clear maximum at $\mu = 0.18$.

the background amplitude μ that include the maximum of CC and the saturation state for a fixed value of the time variable $\zeta(t)$. The peak indicates the range of values for the background modulating the rogue wave, sometimes called the "gradient catastrophe" [57].

4. Conclusion

We have studied one-soliton and rogue wave solutions propagating in Ablowitz-Ladik waveguides modeled with the discrete nonlinear Schrödinger equation, using a measure of space complexity known as Configurational Complexity (CC). For discrete solitons, the configurational complexity displays plateaus for dif-

ferent values of the transverse parameter κ as it evolves in time, with a sharp minimum in between (see Fig. 1). Using the interpretation of the CC measure, the high plateaus imply that there is more spatial localization and momentum modes contributing similarly to the object without much gain or loss of efficiency in information storage. A minimum in CC indicates stability, where there is less spatial compression and a larger number of modes contribute similarly to the modal fraction, allowing for more information encoding. For rogue waves, we found that the CC displays both saturation for larger times for illustrative values of the amplitude modulation parameter μ (see Fig. 3), as well as a clear maximum for a time snapshot at $\mu = 0.18$ (see Fig. 4). The saturation indicates the dispersion of the configuration into free waves, while the maximum indicates maximum spatial compression for the optimal modulation amplitude triggering the onset of such unstable waves.

We plan to expand this study to objects in higher dimensions in future work, as well as offer a more detailed parameter analysis. We hope our results will inspire further work on the application of entropic measures to discrete and continuous solitons with the goal of aiding the design of more efficient Ablowitz-Ladik waveguides and other solitonic conduits.

CRediT authorship contribution statement

Pooja Thakur and Prof. Marcelo Gleiser have equal contribution in framing the problem and getting its mathematical solutions. Prof. Marcelo Gleiser provided the graphical explanation of Configurational Complexity. The critical evaluation of the manuscript and explanation has been provided by Prof. Marcelo Gleiser.

Declaration of competing interest

The authors declare that they have no known competing financial interests or personal relationships that could have appeared to influence the work reported in this paper.

Acknowledgement

The financial support from Department of Science and Technology, New Delhi through Women Scientist Scheme-A project (Ref. No. SR/WOS-A/PM-109/2017G) is gratefully acknowledged by Pooja Thakur. P. Thakur and R. Gupta thank Prof. C.N. Kumar, Department of Physics, Panjab University, Chandigarh for many useful discussions.

References

[1] P.G. Kevrekidis, The Discrete Nonlinear Schrödinger Equation, Springer-Verlag, Heidelberg, 2009.
[2] C. Sulem, P.L. Sulem, The Nonlinear Schrödinger Equation, Springer-Verlag, New York, 1999.
[3] M.J. Ablowitz, B. Prinari, A.D. Trubatch, Discrete and Continuous Nonlinear Schrödinger Systems, Cambridge University Press, Cambridge, 2004.
[4] P.G. Kevrekidis, D.J. Frantzeskakis, R. Carretero-Gonzalez, The Defocusing Nonlinear Schrödinger Equation: From Dark Solitons to Vortices and Vortex Rings, SIAM, Philadelphia, 2015.
[5] D.N. Christodulides, F. Lederee, Y. Silberberg, Nature 424 (2003) 817.
[6] A.A. Sukhorukov, Y.S. Kivshar, H.S. Eisenberg, Y. Silberberg, IEEE J. Quantum Electron. 39 (2003) 31.
[7] F. Lederer, G.I. Stegeman, D.N. Christodulides, G. Assanto, M. Segev, Y. Silberberg, Phys. Rep. 463 (2008) 1.
[8] O. Morsch, M. Oberthaler, Rev. Mod. Phys. 78 (2006) 179.
[9] M. Peyrard, Nonlinearity 17 (R1) (2004).
[10] C. Chong, P.G. Kevrekidis, Coherent Structure in Granular Crystal: From Experiment and Modeling to Computation and Mathematical Analysis, Springer-Verlag, Heidelberg, 2018.
[11] A.K. Sieradzan, A. Niemi, X. Peng, Phys. Rev. E 90 (2004) 062717.
[12] A.J. Seivers, S. Takeno, Phys. Rev. Lett. 86 (2001) 2353.
[13] E. Hecht, Optics, 4th edition, Addison Wesley, 2001, ISBN-13 9780805385663.
[14] J. Cuevas-Maraver, P.G. Kevrekidis, B.A. Malomed, L. Guo, J. Phys. A, Math. Theor. 52 (2019) 065202.
[15] A. Ankiewicz, N. Akhmediev, J.M. Soto-Crespo, Phys. Rev. E 82 (2010) 026602.
[16] Y. Ohta, J. Yang, J. Phys. A, Math. Theor. 47 (2014) 255201.
[17] T. Kapitula, P.G. Kevrekidis, Nonlinearity 14 (2001) 533.
[18] D. Cai, A.R. Bishop, N. Grønbech-Jensen, M. Salerno, Phys. Rev. Lett. 74 (1995) 1186.
[19] L.F. Mollenauer, R.H. Stolen, J.P. Gordan, Phys. Rev. Lett. 45 (1980) 1095.
[20] D.N. Christodoulides, R.I. Joseph, Opt. Lett. B 13 (1988) 794.
[21] D. Neshev, et al., Opt. Lett. B 29 (2004) 486.
[22] D.R. Solli, C. Ropers, P. Koonath, B. Jalali, Nature (London) 450 (2007) 1054.
[23] D.R. Solli, C. Ropers, B. Jalali, Phys. Rev. Lett. 101 (2008) 233902.
[24] B. Kibler, et al., Nat. Phys. 6 (1) (2010).
[25] V.B. Efimov, A.N. Ganshin, G.V. Kolmakov, P.V.E. McClintock, L.P. Mezhov-Deglin, Eur. Phys. J. Spec. Top. 185 (2010) 181.
[26] W.M. Moslem, P.K. Shukla, B. Eliasson, Europhys. Lett. 96 (2011) 25002.
[27] Y.V. Bludov, V.V. Konotop, N. Akhmediev, Phys. Rev. A 80 (2009) 033610.
[28] M. Shats, H. Punzmann, H. Xia, Phys. Rev. Lett. 104 (2010) 104503.
[29] M. Salerno, Phys. Rev. A 46 (1992) 6856.
[30] C.E. Shannon, W. Weaver, The Mathematical Theory of Communication, University of Illinois Press, Urbana, 1949.
[31] M. Gleiser, N. Stamatopoulos, Phys. Lett. B 713 (2012) 304, arXiv:1111.5597.
[32] M. Gleiser, D. Sowinski, Phys. Rev. D 98 (2018) 056026.
[33] M. Gleiser, N. Stamatopoulos, Phys. Rev. D 86 (2012) 045004, arXiv:1205.3061.
[34] M. Gleiser, N. Jiang, Phys. Rev. D 92 (2015) 044046.
[35] M. Gleiser, D. Sowinski, Phys. Lett. B 772 (2015) 471.
[36] A.E. Bernardini, N.R.F. Braga, R. da Rocha, Phys. Lett. B 765 (2017) 81.
[37] M. Gleiser, D. Sowinski, Phys. Lett. B 727 (2013) 217.
[38] N.R.F. Braga, R. da Rocha, Phys. Lett. B 767 (2017) 386.
[39] C.O. Lee, Phys. Lett. B 772 (2017) 471.
[40] R. Casadio, R. da Rocha, Phys. Lett. B 763 (2016) 434.
[41] G. Karapetyan, Europhys. Lett. 125 (2019) 58001.
[42] M. Gleiser, M. Stephens, D. Sowinski, Phys. Rev. D 97 (2018) 096007.
[43] N.B. Cendjas, R.C. Fuentevilla, A.H. Aguilar, R.R.M. Luna, R. da Rocha, Phys. Lett. B 782 (2018) 607.
[44] A.E. Bernardini, R. da Rocha, Phys. Lett. B 796 (2019) 107.
[45] M. Gleiser, N. Graham, Phys. Rev. D 89 (2014) 083502, arXiv:1401.6225.
[46] N.R.F. Braga, L.F. Ferreira, R. da Rocha, Phys. Lett. B 787 (16) (2018).
[47] R.A. Correa, A. de Souza Dutra, M. Gleiser, Phys. Lett. B 737 (2014) 388.
[48] A. Goncalves da Silva, R. da Rocha, Phys. Lett. B 774 (2017) 98.
[49] B. Rumpf, Phys. Rev. E 77 (2008) 036606.
[50] P. Thakur, M. Gleiser, A. Kumar, R. Gupta, Phys. Lett. A 384 (2020) 126461.
[51] J.C. Eilbeck, P.S. Lomdahl, A.C. Scott, Physica D 16 (1985) 318.
[52] M.J. Ablowitz, J.F. Ladik, Stud. Appl. Math. 55 (1976) 213.
[53] M.J. Ablowitz, J.F. Ladik, J. Math. Phys. 17 (1976) 1011.
[54] Z. Yan, D. Jiang, J. Math. Anal. Appl. 395 (2012) 542.
[55] K. Narita, J. Phys. Soc. Jpn. 59 (1990) 3528.
[56] R.A.C. Correa, D.M. Dantas, P.H.R.S. Moraes, C.A.S. Almeida, Ann. Phys. (Berlin) 1700188 (2017).
[57] R.H.J. Grimshaw, A. Tovbis, Proc. R. Soc. A 469 (20130094) (2013), https://doi.org/10.1098/rspa.2013.0094.